Stochastic Coupled Oscillator Model of EEG for Alzheimer's Disease

P. Ghorbanian[1], S. Ramakrishnan[1], and H. Ashrafiuon[1]

Abstract— **Coupled nonlinear oscillator models of EEG signals during resting eyes-closed and eyes-open conditions are presented based on Duffing–van der Pol oscillator dynamics. The frequency and information entropy contents of the output of the nonlinear model and the actual EEG signal is matched through an optimization algorithm. The framework is used to model and compare EEG signals recorded from Alzheimer's disease (AD) patients and age-matched healthy controls (CTL) subjects. The results show that 1) the generated model signal can capture the frequency and information entropy contents of the EEG signal with very similar power spectral distribution and non-periodic time history; 2) the EEG and the generated signal from the eyes-closed model are α band dominant for CTL subjects and θ band dominant for AD patients; and 3) statistically distinct models represent the EEG signals from AD patients and CTL subject during resting eyes-closed condition.**

I. Introduction

Alzheimers disease (AD) is the most common form of brain disorder among older people. While no known cure exists, a few medications have shown promise in delaying its symptoms [1] prompting researchers to seek early diagnosis and intervention strategies. Electroencephalograph (EEG) recording and signal processing is a potential non-invasive tool that may aid early diagnosis of AD. However, the use of EEG signal analysis to aid the diagnosis of AD is a complex problem and current methods require significant improvement [2].

There are several approaches to the EEG signal analysis with Fast Fourier Transform (FFT) being the most widely method [2]–[4]. Another popular approach suitable for EEG signal processing is wavelet transform since it provides both frequency and time information for the transient signal [5]. However, all these methods are based on linear transformation and cannot capture the nonlinear properties of EEG signals [6]. Hence, nonlinear approaches have been introduced to capture the EEG nonlinear properties mainly through computationally complex time series analysis [7]. Examples of nonlinear approaches include neural mass model [8], coupled oscillators [9], nonlinear non-stationary model [10], random neural networks [11], and chaotic phenomena [12].

Limit cycle oscillators [13], [14] have also been considered in EEG modeling which suggest that a stochastic limit cycle behavior represents the EEG signal better than a description based on chaotic phenomena. Motivated by these studies and preliminary results from our stochastic coupled oscillators [15], we present a framework to model the EEG signal as the stochastic response of a coupled nonlinear oscillator system. Specifically, the EEG signal is modeled as the output of a coupled Duffing - van der Pol oscillator [16], [17].

We present a novel framework to study the EEG, modeling the signal as the stochastic response of a coupled nonlinear oscillator system. Preliminary results [15] has shown that a coupled nonlinear Duffing oscillator model with only two degrees of freedom can capture the linear characteristics of the EEG signal in the major brain EEG frequency bands. However, they also highlighted the need for improved models that can generate outputs to match actual EEG data with reference to nonlinear metrics. Hence, a coupled system of Duffing - van der Pol oscillators [16], [17] is proposed and analyzed in this study.

The procedure is as follows. A global optimization algorithm is employed to match the output of the stochastic ordinary differential equation (ODE) model with each EEG signals in terms of power spectrum and information content as measured by Shannon entropy [18]. The model parameters representing AD patients are then compared with those of healthy controls (CTL) in order to establish statistical significant distinct models for AD and CTL under resting eyes-closed (EC) and eyes-open (EO) conditions.

II. Methods

A. EEG data and Signal Processing

The EEG data used in this study are from an approved pilot study of AD patients versus age matched health control (CTL) subjects [19]. The recording device is a single-dry electrode at Fp1 (based on a 10-20 electrode placement system). The effective sample rate of the device is 125 Hz and its reliable frequency range is 2-30 Hz. Artifacts are removed from the EEG data using an artifact detection algorithm [19]. EEG recording blocks of 40-second duration which provides approximately 5000-sample signals are selected for analysis. In all, 60 random blocks are selected from the pilot study: 40 blocks from CTL subjects (20 EC and 20 EO) and 20 blocks from AD patients (10 EC and 10 EO).

Two measures are used to quantify the EEG signal properties: power spectrum and Shannon entropy. Short time FFT with sliding window is performed on the EEG signal and the time-varying power spectrum corresponding to major brain frequency band are calculated as a linear measure. The power spectrum is computed in seven bands, including the lower δ (1 – 2 Hz), upper δ (2 – 4 Hz), θ (4 – 8 Hz), α (8 – 13 Hz), lower β (13 – 20 Hz), upper β (20 – 30 Hz), and γ (30 – 60 Hz). γ and lower δ bands are ignored since they are unreliable and possess little power. Shannon entropy is

[1]P. Ghorbanian, S. Ramakrishnan, and H. Ashrafiuon are with Center for Nonlinear Dynamics and Control, Villanova University, Villanova, PA 19085 hashem.ashrafiuon@villanova.edu

978-1-4244-7929-0/14/$26.00 ©2014 IEEE

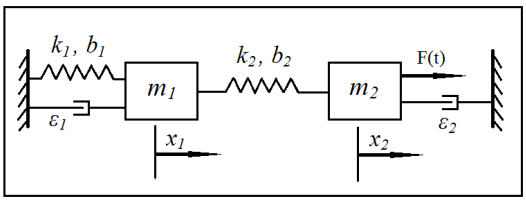

Fig. 1. Schematic of the coupled Duffing–van der Pol oscillators.

used as a nonlinear measure representing predictability and complexity of the EEG signal [20].

B. The Coupled Duffing - van der Pol Oscillators Model

EEG is modeled as the output of a coupled system of two Duffing - van der Pol oscillators subject to white noise excitation, as shown in 1. The equations of motion of the system may be written as:

$$\begin{cases} \ddot{x}_1 + (k_1 + k_2)x_1 - k_2 x_2 = -b_1 x_1^3 \\ \qquad -b_2(x_1 - x_2)^3 + \epsilon_1 \dot{x}_1(1 - x_1^2), \\ \ddot{x}_2 - k_2 x_1 + k_2 x_2 = b_2(x_1 - x_2)^3 \\ \qquad +\epsilon_2 \dot{x}_2(1 - x_2^2) + \mu \; dW, \end{cases} \tag{1}$$

where x_1, $\dot{x_1}$, $\ddot{x_1}$ and x_2, $\dot{x_2}$, $\ddot{x_2}$ are positions, velocities and accelerations of the two oscillators, respectively. Parameters k_1, b_1, ϵ_1 and k_2, b_2, ϵ_2 are, respectively, linear stiffness, cubic stiffness, and van der Pol damping coefficient of the two oscillators. Parameter μ represents the intensity of white noise and dW is a Wiener process [21] representing the additive noise in the stochastic differential system.

C. Optimization Formulation

A global optimization search method based on a multi-start algorithm [22] is emplyed to determine the oscillator model parameters. We selected the velocity of the second mass as the output of our model. The cost function is the weighted average of the root mean squared of the errors in power spectrum of selected brain frequency bands and error in Shannon entropy. Hence, the cost function J is written as:

$$\min_p J = \sqrt{\sum_{j=1}^{m} (P_{Ej} - P_{Oj})^2} + w|S_E - S_O|, \tag{2}$$

where $p = [k_1, k_2, b_1, b_2, \epsilon_1, \epsilon_2, \mu]$ represents the decision variables, P_{Ej} and P_{Oj} are the powers in the major brain frequency bands, m is number of frequency bands ($m = 7$), and S_E and S_O are the Shannon entropies of the EEG signal and the model output, respectively, and w is a weighting factor. Note that, the magnitude of the EEG and output signals are normalized with respect to their standard deviations.

The optimization problem is subject to constraints represented by the state equations and lower and upper bounds for the decision variable which are defined as:

$$\begin{gathered} 0 \le \mu \le 2, \quad 0 < k_i \le 1e4, \; 0 < b_i \le \tfrac{1}{2} k_i, \\ 0 < \epsilon_i \le \tfrac{1}{3} k_i, \; i = 1, 2. \end{gathered} \tag{3}$$

The constraints for b_i and ϵ_i were imposed in order to avoid the chaotic regime [23]. Practically, these constraints maintain a periodic response for the deterministic system when $\mu = 0$. Noise intensity is also constrained to avoid a response dominated by random noise. The initial guesses for the global optimization search are randomly generated within the bounds defined in Eqn. (3).

TABLE I

OPTIMAL MODEL PARAMETERS FOR CTL.

Parameter	EC	EO
k_1	1,345.5 ± 282.2	6,308.1 ± 79.9
k_2	4,255.4 ± 593.9	3,742.0 ± 96.2
b_1	40.78 ± 19.7	196.9 ± 8.0
b_2	296.7 ± 39.7	310.31 ± 37.5
ϵ_1	283.55 ± 30.8	1,496.1 ± 16.4
ϵ_2	2.50 ± 1.2	5.19 ± 0.6

TABLE II

OPTIMAL MODEL PARAMETERS FOR AD.

Parameter	Eyes-Closed (EC)	Eyes-Open (EO)
k_1	6,028.7 ± 93.7	6,123.9 ± 112.5
k_2	3,722.2 ± 198.1	3,800.1 ± 440.7
b_1	194.8 ± 0.2	202.5 ± 13.6
b_2	317.1 ± 7.6	300.65 ± 25.6
ϵ_1	1,478.7 ± 22.7	1,510.2 ± 47
ϵ_2	4.99 ± 0.005	5.2 ± 0.5

III. RESULTS

In order to reduce computation complexity, the optimization algorithm is employed in two stages. First, the noise-free deterministic model is optimized to capture the frequency content and limit cycle characteristics of the EEG blocks. Next, the noise interaction is optimized to capture the information content and predictability of the EEG blocks.

A. Deterministic Model

The self-excited, deterministic Duffing–van der Pol system is considered first, i.e. $\mu = 0$. Using the global optimization algorithm with cost function of Eqn. (2) with $w = 0$ subject to constraints in Eqn. (1) and Eqn. (3), the optimal model parameters are derived for each of the 60 EEG block. The mean and standard deviation of the optimal values of model parameters for the 40 blocks from CTL subjects are presented in Table I and for the 20 blocks from AD patients in Table II.

The mean and standard deviation of the frequency band powers for the optimal model and EEG signals show good agreement for CTL and AD subjects, as presented in Tables III and IV for EC and EO cases, respectively. The comparison reveals that for CTL subjects, the model is closely following the α-band dominance in the EC cases [24]. While, in the EO cases, the model and EEG follow a more flat frequency distribution from upper δ to lower β frequency bands. Furthermore, the model and EEG signal are θ-band dominated in the EC cases for AD patients as previously reported [19]. Another interesting observation is that the difference between frequency content of EC and EO EEG of AD patients is not as clear as it is for CTL subjects.

TABLE III

BRAIN BAND POWERS FOR EC CASE.

Freq. Band	EEG CTL	Model CTL	EEG AD	Model AD
δ_{L}	.02 ± .01	.00 ± .00	.04 ± .03	.00 ± .00
δ_{U}	.08 ± .04	.10 ± .02	.15 ± .04	.17 ± .02
θ	.20 ± .05	.19 ± .06	.40 ± .06	.41 ± .05
α	.49 ± .10	.50 ± .09	.21 ± .05	.27 ± .03
β_{L}	.12 ± .03	.17 ± .06	.10 ± .02	.10 ± .04
β_{U}	.05 ± .02	.03 ± .02	.05 ± .02	.05 ± .01
γ	.02 ± .01	.00 ± .00	.02 ± .01	.01 ± .00

TABLE IV

BRAIN BAND POWERS FOR EO CASE.

Freq. Band	EEG CTL	Model CTL	EEG AD	Model AD
δ_{L}	.05 ± .03	.00 ± .00	.04 ± .04	.00 ± .00
δ_{U}	.15 ± .05	.14 ± .02	.18 ± .08	.18 ± .03
θ	.27 ± .04	.30 ± .04	.33 ± .04	.38 ± .09
α	.23 ± .04	.29 ± .06	.22 ± .09	.28 ± .08
β_{L}	.17 ± .04	.20 ± .04	.11 ± .03	.11 ± .03
β_{U}	.10 ± .05	.05 ± .01	.08 ± .03	.05 ± .01
γ	.03 ± .02	.01 ± .01	.03 ± .01	.01 ± .00

This makes it more difficult to derive statistically significant distinct oscillator models of EC and EO EEG signals for AD patients.

1) Statistical Analysis: An essential objective of our approach is to be able to establish a statistically significant correspondence between variations in model parameters and the variations in actual data due to state and health of the brain. Hence, the statistical significance of differences between model parameters of the EC and EO EEG recordings of AD patients and CTL subjects is assessed. Two methods, t-test and non-parametric Wilcoxon rank sum test, are employed for univariate statistical analysis since the normality test is not consistently satisfied. In the EC case, all model parameter differences between AD and CTL subjects are found to be statistically significance except b_2. However, only k_1 is found to be statistically significance in the EO case. Therefore, the coupled Duffing–van der Pol model is more effective in distinguishing between AD patients and CTL subjects when EC EEG recordings are used.

Next, a power analysis is conducted to determine the influence of the sample size on the statistical testing results between AD and CTL [25]. The results for powers of 90%, 95%, 99%, and 99.9% are listed in Table V for EC cases. The actual difference between means are presented within parentheses following each parameter. Thus, the EC sample size is sufficient for parameter k_1 with more than 99% power, for b_1, ϵ_1, and ϵ_2 with more than 99.9% power, and for k_2 with less than 90% power. Note that, the t-test did not show b_2 to be statistically significant and thus the power confidence need not be established. For the EO case, the testing results was significant only for k_1 with more than 99% of power.

TABLE V

REQUIRED MEAN DIFFERENCE FOR EC.

Parameter	90 %	95 %	99 %	99.9 %
Δ_{k1} (4674)	346	385	457	540
Δ_{k2} (533)	727	810	961	1136
Δ_{b1} (154)	24	26	31	37
Δ_{b2} (20)	49	53	63	75
Δ_{ϵ_1} (1195)	41	46	55	65
Δ_{ϵ_2} (2.4)	1.5	1.7	2.0	2.4

B. Stochastic Model

Preliminary results from our recent work [15] as well as other literature [26], [27] suggest that the EEG must be treated as a stochastic signal. Hence, the optimization procedure is carried out with respect to the intensity of the external white noise excitation while keeping other model parameters equal to the values derived in the deterministic case. Also, Shannon entropy is taken into account using the optimization cost function of Eq. (2) with $w = 0.2$.

The optimal noise intensity for models of the CTL subjects are derived as 1.1 ± 0.36 for EC and 0.49 ± 0.28 for EO. The corresponding Shannon entropy of the output signals are derived as 1.93 ± 0.12 for EC and 1.72 ± 0.09 for EO compared with the actual EEG Shannon entropies of 1.79 ± 0.08 for EC and 1.71 ± 0.11 for EO EEG recordings. Similarly, the optimal noise intensity for models of the AD patients are derived as 0.36 ± 0.1 for EC and 0.33 ± 0.12 for EO. The corresponding Shannon entropy of the output signals are derived as 1.74 ± 0.09 for EC and 1.79 ± 0.07 for EO compared with the actual EEG Shannon entropies of 1.78 ± 0.03 for EC and 1.63 ± 0.32 for EO EEG recordings. The noise intensity model difference between AD and CTL subjects for EC cases are found to be statistically significant with p-value of 0.002 and .004 for t-test and non-parametric test, respectively.

C. Signal Comparisons

Sample EC EEG power spectrum power and those of the outputs of the optimal deterministic and stochastic oscillator models are shown in Fig. 2 for a CTL subject. These plots demonstrate that for the CTL subject, the EC is α band dominated. Note that, the deterministic model has resonance peaks repeated at very discrete frequencies while the stochastic model has a broader frequency distribution similar to the actual signal.

IV. CONCLUSION

We presented EEG signal modeling through stochastic coupled nonlinear oscillators. The results showed that our framework can capture frequency and information entropy contents of actual EEG signal in resting EC and EO conditions. We further applied the technique to EEG signals from AD patients and CTL subjects and showed that the method can provide distinct models with statistically significant parameters under resting EC condition. However, due to flat distribution of the frequency content of EEG signal in EO conditions, the framework did not yield distinct EO models.

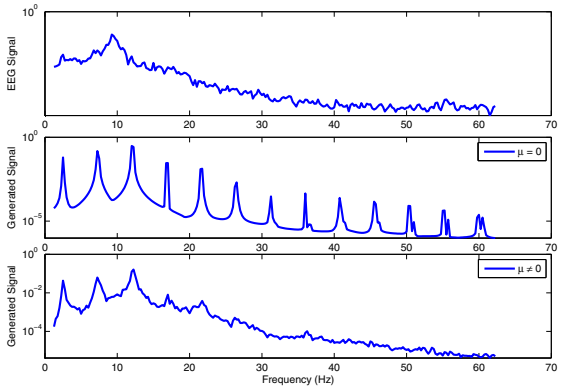

Fig. 2. Power spectrum of a sample CTL subject EC EEG signal (top), deterministic model (middle), and stochastic model (bottom).

The power spectrum comparison showed that the generated signal from the EC model is α dominant for CTL subject and θ dominant for AD patients, as observed in the actual EEG signal. In summary, the results show that the stochastic nonlinear dynamic modeling of EEG signal has the potential to aid in early diagnosis of Alzheimer's disease.

REFERENCES

[1] J. Dauwels, F. Vialatte, and A. Cichocki. Diagnosis of Alzheimer's disease from EEG signals: where are we standing. *Current Alzheimer Research*, 7(6):487 – 505, 2010.

[2] M. Elgendi, F. Vialatte, A. Cichocki, C. Latchoumane, J. Jeong, and J. Dauwels. Optimization of EEG frequency bands for improved diagnosis of Alzheimer disease. In *Int. Conf. of the IEEE Eng. in Medicine and Biology Society*, pages 6087 – 6091, Boston, MA, August 2011.

[3] C. Huang, L.-O. Wahlund, T. Dierks, P. Julin, B. Winblad, and V. Jelic. Discrimination of Alzheimer's disease and mild cognitive impairment by equivalent EEG sources: a cross-sectional and longitudinal study. *Clinical Neurophysiology*, 111(11):1961 – 1967, November 2000.

[4] K. Bennys, G. Rondouin, C. Vergnes, and J.B. Touchon. Diagnostic value of quantitative EEG in Alzheimer's disease. *Clinical Neurophysiology*, 31(3):153 – 160, June 2001.

[5] T. Bassani and J. C. Nievola. Pattern recognition for brain-computer interface on disabled subjects using a wavelet transformation. In *IEEE Symposium on Computational Intelligence in Bioinformatics and Computational Biology*, pages 180 – 186, Sun Valley, USA, September 2008.

[6] M. Akin. Comparison of wavelet transform and FFT methods in the analysis of EEG signals. *Journal of Medical Systems*, 26(3):241–247, June 2002.

[7] J. Jeong. EEG dynamics in patients with Alzheimer's disease. *Clinical Neurophysiology*, 15(7):1490–1505, July 2004.

[8] G. Huang, D. Zhang, J. Meng, and X. Zhu. Interactions between two neural populations: A mechanism of chaos and oscillation in neural mass model. *Neurocomputing*, 74(6):1026 – 1034, February 2011.

[9] L. Leistritz, P. Putsche, K. Schwab, W. Hesse, T. Susse, J. Haueisen, and H. Witte. Coupled oscillators for modeling and analysis of EEG/MEG oscillation. *Biomed Tech*, 52(1):83 – 89, February 2007.

[10] L. Rankine, N. Stevenson, M. Mesbah, and B. Boashash. A nonstationary model of newborn EEG. *IEEE Transactions on Biomedical Engineering*, 54(1):19 – 28, January 2007.

[11] L. Acedo and J.A. Morano. Brain oscillations in a random neural network. *Mathematical and Computer Modeling*, 57(7):1768 – 1772, 2013.

[12] M.P. Dafilis, F. Frascoli, P.J. Cadusch, and D.T.J. Liley. Chaos and generalised multistability in a mesoscopic model of the electroencephalogram. *Physica D: Nonlinear Phenomena*, 238(13):1056 – 1060, 2009.

[13] J.L. Hernandez, P.A. Valdes, and P. Vila. EEG spike and wave modeled by a stochastic limit cycle. *Neuroreport.*, 7(13):2246 – 2250, September 1996.

[14] D.P. Burke and A.M. De Paor. A stochastic limit cycle oscillator model of the EEG. *Biological Cybernetics*, 91(4):221 – 230, October 2004.

[15] P. Ghorbanian, S. Ramakrishnan, A.J. Simon, and H. Ashrafiuon. Stochastic dynamic modeling of the human brain EEG signal. In *ASME Dynamic Systems and Control Conference*, Palo Alto, CA, October 2013.

[16] A. Kimiaeifar, A.R. Saidi, G.H. Bagheri, M. Rahimpour, and D.G. Domairry. Analytical solution for Van der Pol-Duffing oscillators. *Chaos, Solitons and Fractals*, 42(5):2660–2666, December 2009.

[17] E. Camacho, R. Rand, and H. Howland. Dynamics of two van der pol oscillators coupled via a bath. *International Journal of Solids and Structures*, 41:2133 – 2143, 2004.

[18] C.E. Shannon. A mathematical theory of communication. *The Bell System Technical Journal*, 27:379 – 423 , 623 – 656, October 1948.

[19] P. Ghorbanian, D.M. Devilbiss, A. Verma, A. Bernstein, T. Hess, A.J. Simon, and H. Ashrafiuon. Identification of resting and active state EEG features of Alzheimers disease using discrete wavelet transform. *Annals of Biomedical Engineering*, 41(6):1243 – 1257, June 2013.

[20] H.C. Shin, S. Tong, S. Yamashita, X. Jia, R.G. Geocadin, and N.V. Thakor. Quantitative EEG and effect of hypothermia on brain recovery after cardiac arrest. *IEEE Transactions on Biomedical Engineering*, 53(6):1016 – 1023, June 2006.

[21] D. J. Higham. An algorithmic introduction to numerical simulation of stochastic differential equations. *SIAM Review*, 43(3):525 – 546, 2001.

[22] Z. Ugray, L. Lasdon, J. Plummer, F. Glover, J. Kelly, and R. Marti. Scatter search and local nlp solvers: A multistart framework for global optimization. *INFORMS Journal on Computing*, 19(3):328 – 340, July 2007.

[23] Z. Li, W. Xu, and X. Zhang. Analysis of chaotic behavior in the extended duffing-van der pol system subject to additive non-symmetry biharmonical excitation. *Applied Mathematics and Computation*, 183(2):858 – 871, December 2006.

[24] S. Sanei and J. A. Chambers. *EEG signal processing*. John Wiley and Sons, West Sussex, England, 2007.

[25] J. L. Devore. *Probability and Statistics for Engineering and the Sciences*. Thomson Brooks/Cole, Belmont, CA, 2004.

[26] J. Fell, A. Kaplan, B. Darkhovsky, and J. Roschke. EEG analysis with nonlinear deterministic and stochastic methods: a combined strategy. *Acta Neurobiologiae Expermentails*, 60(1):87 – 108, 2000.

[27] S. Sun, M. Lan, and Y. Lu. Adaptive EEG signal classification using stochastic approximation methods. In *Int. Conf. on Acoustics, Speech and Signal Process*, pages 413 – 416, Las Vegas, NV, April 2008.